Published in final edited form as:
Cancer Res. 2008 September 1; 68(17): 7090–7099. doi:10.1158/0008-5472.CAN-08-0643.

Thrombospondin-1 promotes tumor macrophage recruitment and enhances tumor cell cytotoxicity of differentiated U937 cells

Gema Martin-Manso[1], **Susana Galli**[1], **Lisa A. Ridnour**[2], **Maria Tsokos**[1], **David A. Wink**[2], and **David D. Roberts**[1,*]

1*Laboratory of Pathology, Center for Cancer Research, National Cancer Institute, National Institutes of Health, Bethesda, Maryland 20892*

2*Radiation Biology Branch, Center for Cancer Research, National Cancer Institute, National Institutes of Health, Bethesda, Maryland 20892*

Abstract

Inhibition of tumor growth by thrombospondin-1 (TSP1) is generally attributed to its anti-angiogenic activity, but effects on tumor immunity should also be considered. We show that over-expression of TSP1 in melanoma cells increases macrophage recruitment into xenograft tumors grown in nude or beige/nude mice. In vitro, TSP1 acutely induces expression of plasminogen activator inhibitor-1 (PAI-1) by monocytic cells, suggesting that TSP1-induced macrophage recruitment is at least partially mediated by PAI-1. Tumor-associated macrophages can either promote or limit tumor progression. The percentage of M1 polarized macrophages expressing inducible nitric oxide synthase is increased in TSP1-expressing tumors. Furthermore, soluble TSP1 stimulates killing of breast carcinoma and melanoma cells by interferon-γ-differentiated U937 cells *in vitro* via release of reactive oxygen species. TSP1 causes a significant increase in phorbol ester-mediated superoxide generation from differentiated monocytes by interaction with α6β1 integrin through its N-terminal region. The N-terminal domain of thrombospondin-2 also stimulates monocyte superoxide production. Extracellular calcium is required for the TSP1-induced macrophage respiratory burst. Thus, TSP1 may play an important role in anti-tumor immunity by enhancing recruitment and activation of M1 tumor-associated macrophages, which provides an additional selective pressure for loss of TSP1 and thrombospondin-2 expression during tumor progression.

Keywords

thrombospondin-1; plasminogen activator inhibitor-1; integrins; superoxide anion; tumor-associated macrophages

Introduction

Thrombospondin-1 (TSP1) is a secreted glycoprotein that is predominantly stored in platelets but also secreted at low levels by many cell types including monocytes and macrophages. TSP1 is rapidly and transiently released in response to tissue injury and is elevated in several chronic diseases (1,2). TSP1-null mice display acute and chronic inflammatory pulmonary infiltrates, and an elevated number of circulating white blood cells (3), suggesting an anti-inflammatory

*To whom correspondence should be addressed: David D. Roberts NIH, Building 10, Room 2A33 10 Center Dr. MSC 1500, Bethesda, MD, 20892 Telephone: (301) 496 6264 E-mail: droberts@helix.nih.gov

Disclosures
None.

role. In contrast, TSP1 expression in ischemic injuries limits tissue survival and restoration of perfusion by blocking NO/cGMP signaling (4). The diverse biological activities of TSP1 are mediated by its multiple functional domains that engage corresponding receptors expressed by a variety of cells. Differential expression or activation of cell surface receptors for TSP1 including integrins, CD36, CD47, low density lipoprotein (LDL) receptor-related protein, proteoglycans, and sulfatides may dictate the specific responses of each cell type to TSP1 (5).

TSP1 plays several roles in the physiological functions of phagocytes. TSP1 mediates phagocytosis of neutrophils undergoing apoptosis (6). Macrophage recognition and phagocytosis of apoptotic fibroblasts requires fibroblast-derived TSP1 and CD36 (7). CD36-deficient patients have impaired oxidized LDL-induced NFκB activation and subsequent cytokine expression (8). TSP1 modulates expression of IL-6 and IL-10 by monocytes (9) and activation of latent TGFβ (3). TSP1 stimulates motility of human neutrophils (10,11) and promotes chemotaxis and haptotaxis of human peripheral blood monocytes (12). In addition, TSP1 enhances cytokine-induced respiratory burst of human neutrophils (13) and enhances chemoattractant FMLP-mediated superoxide anion (O_2^-) generation by human neutrophils through its N-terminal domain (14,15). However, the underlying mechanism for regulation of O_2^- generation has not been delineated. Here, we provide evidence that soluble TSP1 causes a significant increase in phorbol 12-myristate 13-acetate (PMA)-mediated O_2^- generation from interferon-γ (IFN-γ)-differentiated human monocytes by interaction with α6β1 integrin through its N-terminal region and identify a requirement for extracellular calcium to mediate the macrophage respiratory burst.

Macrophages are an important effector cell of innate immunity against tumors. However, tumor-associated macrophages (TAMs) can differentiate into either cytotoxic (M1) or tumor growth-promoting (M2) states. This differentiation depends on the tissue microenvironment (16). Macrophages are classically activated toward the M1 phenotype by IFN-γ alone or in concert with microbial products. Alternative activation by stimulation with interleukin (IL)-4 or IL-13, IL-10, IL-21, transforming growth factor-β (TGFβ), immune complexes, and glucocorticoids drives macrophages toward the M2 phenotype (17). M2 macrophages are present in most established tumors and promote tumor progression (18).

TSP1 is often down-regulated during tumor progression and inhibits tumor growth when re-expressed (19). This activity is generally attributed to angiogenesis inhibition, but the above results suggest that effects on tumor immunity should also be considered. The current study demonstrates an important role for TSP1 as a positive modulator of innate anti-tumor immunity by increasing macrophage recruitment and stimulating reactive oxygen species (ROS)-mediated tumor cytotoxicity.

Materials and Methods

Proteins and peptides

Human TSP1 was purified from the supernatant of thrombin-activated platelets obtained from the NIH Blood Bank (20). Recombinant human TSP1 was obtained from EMP Genetech. Recombinant proteins containing various domains of TSP1 and TSP2 were prepared as previously described and provided by Dr. Deane Mosher (21-23). The $\alpha_6\beta_1$ integrin inhibitory peptide (LALERKDHSG) derived from TSP1 and the control peptide (LALARKDHSG) were prepared as described (24). Xanthine, xanthine oxidase and superoxide dismutase (SOD) were obtained from Stratagene.

Reagents

Rat anti-mouse CD68 antibody (clone FA-11) was from AbD Serotec. Monoclonal neutralizing antibody (clone 9016) against human TGFβ1, recombinant human and mouse IFN-γ, recombinant human TGF β1, and recombinant human IL-4 were from R&D Systems. Rabbit polyclonal to plasminogen activator inhibitor type 1 (PAI-1) and rabbit polyclonal to inducible nitric oxide synthase (iNOS) were from Abcam Inc. Anti-actin (Ab-1) mouse monoclonal antibody and EGTA were from Calbiochem. The function-blocking rat anti-human α_6 integrin monoclonal antibody (clone G0H3) was from Chemicon International, Inc. (Temecula, CA). FITC-conjugated rat anti-human α_6 monoclonal antibody (clone G0H3) and the isotype control were from BD Biosciences. LPS from *E.* coli 0111:B4 and PMA were from Sigma-Aldrich. The inhibitor of inducible nitric oxide synthase (iNOS), aminoguanidine, was from Sigma-Aldrich. The $\alpha_4\beta_1$ integrin antagonist (4-((2-methylphenyl) aminocarbonyl) aminophenyl) acetyl-LDVP (25) was obtained from Bachem. The calcium indicator Fluo-4/AM, rabbit polyclonal anti-fluorescein/Oregon Green, and Pluronic F-127 were from Molecular Probes.

THBS1 transfected cells

MDA-MB-435 cells transfected with the *THBS1* expression plasmid (clone TH26, 7.5-fold higher TSP1 expression than control) or the empty pCMVBamNeo vector (Neo) were described previously (26).

Cell culture and differentiation

Transfected MDA-MB-435 cells were cultured at 37 °C, 5% CO_2, in complete RPMI 1640 (Gibco) containing 10% fetal bovine serum (FBS) (Biosource), 2 mM glutamine, 100 units/ml penicillin, 100 μg/ml streptomycin, and 750 μg/ml geneticin (Gibco). The human monocytic line U937 (27) kindly provided by Dr. Mark Raffeld (NCI, NIH, Bethesda, MD) was cultured at 37 °C, 5% CO_2, in RPMI-1640 supplemented with 2 mM glutamine, 100 units/ml penicillin, 100 μg/ml streptomycin, and 10% endotoxin tested FBS (Biosource). For differentiation with IFN-γ, 2.0×10^5 U937cells/ml in complete growth medium containing 1mM sodium pyruvate, 0.1mM MEM with non-essential amino acids (Cellgro), and 100 U/ml recombinant human IFN-γ were incubated for 3 days at 37°C. For differentiation with IL-4, 2.0×10^5 U937 cells/ml in AIM-V + AlbuMAX serum free medium (Gibco) containing 10 ng/ml recombinant human IL-4 were incubated for 3 days at 37°C. MDA-MB-231, MDA-MB-435, and MCF7 cells were cultured in RPMI 1640 containing 10% FBS, 2 mM glutamine, 100 units/ml penicillin, and 100 μg/ml streptomycin. Murine macrophage cell lines ANA-1 (28) and RAW264.7 were cultured in DMEM (Gibco) supplemented with 2 mM glutamine, 100 units/ml penicillin, 100 μg/ml streptomycin, and 5% FBS endotoxin tested (Biosource). Human peripheral blood mononuclear cells (PBMCs) were prepared by gradient centrifugation. In brief, fresh human buffy coat (NIH Blood Bank) was diluted 1/4 with sterile Dulbecco's PBS (Gibco). Human PBMCs were isolated by mixing Lymphocyte Separation Medium 1.077 g/ml (Cambrex) and the diluted human blood and centrifuged 30 min at 900 xg, 18° to 20°C. Human monocytes were isolated from PBMCs by adherence to plastic.

Tumorigenesis assay in nude mice

Groups of 10 female NIH-*bg/nu* mice, approximately 8 weeks of age, were injected in the mammary fat pads with 8×10^5 Neo or TH26 cells. Primary tumor size was determined twice weekly by length × width × height measurement. The primary tumors were removed on week 11.

A total of 15 female NIH-*nu/nu* mice, 7 weeks of age, were subcutaneously injected in the right hind leg with 5×10^6 MDA-MB-435 cells. 5 animals were injected with Neo and 10 with TH26 cells. Primary tumor size was determined twice weekly, and tumor volume was calculated as

(width)^2 × length/2. Primary tumors were removed when the volume was 300-400 mm^3 or at week 7. For histopathological analysis, tumor tissues were fixed in buffered formalin, embedded in paraffin, sectioned (5 μm) and stained with hematoxylin and eosin. Animal experiments were conducted in an accredited facility according to NIH guidelines under a protocol approved by the NCI Animal Care and Use Committee.

Immunohistochemical evaluation

Slides were deparaffinized in xylene (3 times 10 min) and rehydrated in graded alcohol (100%, 95 % and 70%). Antigen retrieval was performed in a pressure cooker containing Target Retrieval Solution, pH 6.10 (Dako Corporation, Carpinteria, CA) for 30 min (CD68 antibody) or 10 min (PAI-1 antibody), or 10 mM Citrate buffer, pH 6.0 for 10 min followed by cooling at RT for 20 min (iNOS antibody), and then washed with PBS two times for 10 min. Endogenous peroxidase activity was quenched by 0.3% H_2O_2 in water. After washing the slides with Wash Buffer Solution (Dako Corporation), non-specific binding was reduced using Protein Block Serum-Free (Dako Corporation) for 10 min. The slides were incubated with CD68 antibody (1:100, overnight at 4 °C), PAI-1 antibody (dilution 1:250, 1 h at RT), iNOS antibody (1:50, 1 h at RT). Slides were than incubated with Streptavidin-biotin (Dako LSBA + Kit, HRP). DAB (3,3 –diaminobenzidine solution - Dako Corporation) was used as chromogen for 5 minutes, and hematoxylin was used for counterstaining. Negative control slides omitted the primary antibody. CD68 was located predominantly within the cells. Nuclei were negative. Cytoplasmic and extracellular staining in macrophages was considered positive for PAI-1. Cytoplasmic staining in macrophages was considered positive for iNOS. The intensity of the staining was evaluated using a Nikon Eclipse E1000 microscope equipped with a micro-color camera (RGB-MS-C). The acquisition software was IPLab-Scientific Image Processing 3.5.5.

Measurement of monocyte chemotactic protein-1 (MCP-1), PAI-1, and IL-10

MCP-1, PAI-1, and IL-10 levels in differentiated U937 cells supernatants were measured with a Multiplexed ELISA array (Quansys Biosciences). All samples were run in replicate.

Western blotting

RAW264.7 cells were serum-deprived for 48 h before addition of TGFβ1 or TSP1. After 2-4 h incubation at 37 °C, 5% CO_2, in AIM-V + AlbuMAX serum free medium (Gibco), cells were lysed at 4°C in 0.5% deoxycholic acid, 0.1% SDS, 50 mM HEPES, 1% Triton X-100, 1% NP-40, 150 mM NaCl, 50 mM NaF, 1 mM sodium orthovanadate, 2 μg/ml aprotinin, 2 μg/ml leupeptin and 1mM PMSF. Cell pellets were vortexed briefly and centrifuged at 14,000 rpm for 15 min. Cell lysates (15 μg protein) were boiled for 5 min in SDS-sample buffer, electrophoretically-separated on NuPAGE 10% Bis-Tris gels (Invitrogen) for 1.5 h at 150V and transferred to Immobilon-P polyvinylidene difluoride membranes (Millipore) for 2 h at 100V. Membranes were blocked in 5% BSA/0.1% Tween 20/PBS and incubated overnight with rabbit polyclonal to PAI-1 (2.5 μg/ml). ECL (Upstate) was used for detection. Stripped membranes were reprobed with actin antibody to confirm protein loading levels.

Real-time quantitative reverse transcription-PCR analysis

Total RNA was extracted from Neo and TH26 tumors using Trizol (Invitrogen), according to the manufacturer's instructions. Total RNA was treated with recombinant DNase I (DNA-free kit, Applied Biosystems) and quantified using the NanoDrop ND-1000 Spectrophotometer (Nano-Drop Technologies). cDNA was synthesized from total RNA using iScript cDNA Synthesis Kit (BioRad). Real-time PCR for mouse iNOS and arginase-1 expression profiling was performed on a 7500 Real Time PCR instrument (Applied Biosystems, Foster City, CA) using Taqman oligonucleotide primers Mm00440485_m1 and Mm00475988_m1,

respectively. Data were normalized against mouse hypoxanthine phosphoribosyltransferase 1 (HPRT1: Mm00446968_1). Relative iNOS and arginase-1 expression was calculated using the $2^{-\Delta\Delta CT}$ method.

U937 and ANA-1 cell-mediated cytolysis

MDA-MB-231, MDA-MB-435, and MCF-7 target cells were seeded into 16-well plates in 150 μl of growth medium. Cell growth was dynamically monitored using RT-CES system (ACEA Biosciences) for 24 h. Differentiated U937 effector cells at an E:T ratio of 40:1 were added into wells containing target cells. ANA-1 cells were activated for 20 h at 37°C with 10 ng/ml of LPS and 100 U/ml of IFN-γ in complete medium and also used at an E:T ratio of 40:1. After addition of effector cells, measurements were automatically collected by the analyzer every 10 min for up to 48 h.

Cytotoxicity assay

MDA-MB-231 cells (2×10^3 cells/well) were seeded into 96-well plates in 200 μl of growth medium in the absence or the presence of soluble TSP1 for up to 72 h at 37°C. MDA-MB-231 (2,500 cells/well) were seeded into 96-well plates in 100 μl of RPMI 1640 containing 1.25 % FBS, 2 mM glutamine, 100 units/ml penicillin, and 100 μg/ml streptomycin in the absence or the presence of xanthine/xanthine Oxidase for 72 h at 37°C. Media were collected to assess lactate dehydrogenase (LDH) released due to cell death. LDH release was quantified using a colorimetric assay (Promega). All samples were run in triplicate.

Superoxide production

O_2^- levels in differentiated U937 and activated ANA-1 cells supernatants were quantified using the LumiMax Superoxide Anion detection kit (Stratagene).

Flow Cytometry analysis

Direct immunofluorescence was performed by incubating 1×10^6 cells with 50 μg/ml of FITC-conjugated rat anti-human α_6 antibody (clone G0H3) or isotype control for 45 min at 4°C in Hank's balanced salt solution (HBSS) containing 0.1% BSA, and 0.1% sodium azide (Sigma-Aldrich). After staining, propidium iodide was added and the cells were analyzed on a FACScan flow cytometer (Becton Dickinson). The analysis software was FlowJo (7.2.1).

Measurement of intracellular free Ca^{2+}

Differentiated U937 cells were incubated with loading solution consisting of HEPES-buffered saline (11.6 mM HEPES (Cellgro) in HBSS), supplemented with 2 μM Fluo-4, 0.02 % Pluronic F-127, and 1% BSA for 30 min and then incubated in loading solution without Fluo-4 for 30 min to allow deesterification of the probe. Loading solution was replaced with HBSS containing anti-fluorescein antibody and TSP1. The cells were then placed in a fluorometer (GENios Plus Tecan), and measurements were collected every 5 min for up to 40 min.

Statistical analysis

All data are shown as mean ± SD except were indicated. Significance was determined with one-tailed distribution Student's *t* test analysis. The difference was considered significant (*) when $P \leq 0.05$, and (**) when $P \leq 0.001$.

Results

TSP1 Over Expression Increases Tumor Macrophage Recruitment *in vivo*

Expression of TSP1 in the melanoma cell line MDA-MB-435 significantly inhibits tumor growth and metastasis (26). Notably, increased infiltration of monocytes was observed in clone TH26 tumors that highly express TSP1 (26) and in tumor-bearing mice treated with TSP1 peptides (29). Because macrophage recruitment into wounds is TSP1-dependent (1) we examined the effect of tumor cell TSP1 over expression on TAM recruitment. Using the previously described conditions of injection in the mammary fat pads (26), we confirmed that TH26 tumors showed delayed growth in female NIH-*bg/nu* mice relative to control-transfected clones (*data not shown*). The primary tumors were removed on week 11, and 7 randomly selected mice were analyzed by immunohistochemistry. TAMs were detectable in non-necrotic areas of tumor stained with Hematoxylin-Eosin (*data not shown*). Based on CD68 antibody staining, the percentage of TAMs was significantly higher in TH26 tumors than in Neo tumors ($p<0.05$; Fig. 1*A*).

Mammary fat pad injection was used previously as an orthotopic model of breast carcinoma growth, but recent studies have confirmed that the MDA-MB-435 cell line is a derivative of the M14 melanoma cell line (30). To determine whether TSP1 suppresses tumor growth at a site more appropriate for melanoma, 15 female NIH-*nu/nu* mice were subcutaneously injected in the right hindlimb with TH26 or Neo cells. TSP1 over-expression in TH26 cells also inhibited subcutaneous tumor growth ($p\leq0.001$; Fig. 1*B*). The primary tumors were removed when the volume was 300-400 mm^3 or at week 7, and analyzed by immunohistochemistry. Sections of tumor were stained with Hematoxylin-Eosin and anti-mouse CD68 antibody. Increased TAM infiltration was observed in subcutaneous TH26 versus Neo tumors ($p<0.001$; Fig. 1*C* and *D*).

Role of MCP-1 and PAI-1 in TSP1-dependent TAM Recruitment

MCP-1 is an important regulator of monocyte recruitment (31), and a deficit in MCP-1 was proposed to account for decreased infiltration of macrophages into an excisional wound of TSP1 null mice (1). However, 12 h of stimulation with different doses of soluble TSP1 resulted in no significant change in total MCP-1 release from differentiated U937 human monocytic cells (Fig. 2*A left*).

Macrophage migration *in vitro* and *in vivo* also depends on PAI-1 (32)(33), and elevated PAI-1 expression was previously reported in TH26 versus Neo cells (34). Therefore, increased PAI-1 could also account for increased TAM recruitment into TH26 tumors. Because this result was obtained using a stable transfectant, it was unclear whether TSP1 directly regulates PAI-1 expression rather than the increased PAI-1 being an indirect adaptation of the transfected clones. Incubation of differentiated U937 cells with TSP1 resulted in an acute dose- and time-dependent increase in PAI-1 expression, with a maximal 50-fold induction at 8 h (Fig. 2*A right-B*, $p<0.001$)). Because PAI-1 is a TGFβ-inducible gene (35) and bioactive TGFβ is present in TSP1 purified from platelets (36), we asked whether TGFβ contamination or TSP1-mediated activation of latent TGFβ (3) contributed to the PAI-1 response in U937 cells. Interestingly, stimulation with 3 μg/ml of soluble recombinant 3TSR, the type 1 repeat domain of TSP1 responsible for the TSP1-mediated activation of latent TGFβ (37), resulted in no significant change in total PAI-1 release from differentiated U937 cells (Fig. 2*B*). Therefore, activation of latent TGFβ probably does not account for the effect of TSP1 on PAI-1 expression. The N-terminal module of TSP1 increases FMLP-mediated O_2^- generation and chemotaxis by human neutrophils (10,14) but also had no effect in PAI-1 expression (*data not shown*).

TSP1 stimulation of PAI-1 production was then examined in the presence of a neutralizing TGFβ1 antibody. At 5 μg/ml the neutralizing antibody partially inhibited TSP1-stimulated PAI-1 production (Fig. 2*C left*). Furthermore, recombinant human TSP1 at the same concentration, which should lack TGFβ contamination, showed less stimulatory activity than platelet TSP1 (Fig. 2*C right*). Therefore, bioactive TGFβ present in platelet TSP1 at least partially mediates the stimulation of PAI-1 production by TSP1, but TSP1 lacking TGFβ is also active.

To address whether TSP1 also induces PAI-1 production in mouse macrophages, we used the RAW264.7 macrophage cell line. Increased PAI-1 expression was detected in whole-cell lysates within 2 h after TGFβ (positive control) or TSP1 treatment (Fig. 2*D left*). Furthermore, increased PAI-1 secretion was detected in cell culture supernatants within 4 h after TGFβ or TSP1 treatment (*data not shown*). We also examined whether PAI-1 is expressed by murine TAMs *in vivo*. Immunohistochemical analysis demonstrated strong PAI-1 staining in the TH26 TAMs (Fig. 2*D right*).

Increased M1 macrophage recruitment into TSP1 over-expressing tumors

Activated murine macrophages metabolize L-arginine via two main pathways that are catalyzed by the inducible enzymes iNOS and arginase. Increased iNOS is characteristic of M1 macrophages, and arginase-1 is a marker of M2 macrophages (38). To compare iNOS expression *in vivo*, total RNA extracted from 6 randomly selected Neo and TH26 tumors was analyzed using real-time PCR. A 3.8-fold increase in iNOS expression was found in TH26 tumors (Fig. 3*A*). In contrast, the M2 marker arginase-1 was equally expressed in both tumors (*data not shown*). Staining of tumor sections using an iNOS antibody showed an increased percentage of iNOS expressing TAMs in TH26 versus Neo tumors ($p \leq 0.001$; Fig. *3B-C*). Taken together, these data demonstrate that M1 cytotoxic macrophages are a minor fraction of the TAMs in MDA-MB-435 tumors, but their recruitment or differentiation is increased when the tumors express TSP1.

To address whether M2 macrophage differentiation or function is sensitive to TSP1 *in vitro*, U937 cells were differentiated using IL-4 for 72 h in the absence or presence of soluble TSP1. IL-10 levels in the cell culture supernatants, a marker of M2 polarization, showed no significant differences (Fig. 3*D left*). Similarly, incubation of IL-4-differentiated U937 cells with soluble TSP1 (20 μg/ml) for 12 h did not alter IL-10 secretion (Fig. 3*D right*).

TSP1 stimulates Macrophage Cytotoxicity towards Breast Carcinoma and Melanoma Cells

To determine whether TSP1 can regulate tumor cell killing by macrophages, we performed dynamic monitoring of macrophage-mediated cytolysis. IFN-γ differentiated U937 cells were incubated with MDA-MB-231 breast carcinoma cells (at an E:T ratio of 40:1) in the RT-CES system. The Cell Index readout assesses changes in viable adherent cells by electrical impedance. Differentiated U937 cells expressed constitutive cytotoxic activity against MDA-MB-231 cells (Fig. 4A). Moreover, tumoricidal activity was increased 5-fold after 18 h incubation with soluble TSP1 (5 μg/ml, Fig. 4*A left*). This concentration of TSP1 did not show any direct cytotoxic activity against MDA-MB-231 cells (Fig. 4*A right*). TSP1 similarly enhanced cytotoxicity against MDA-MB-435 melanoma and MCF-7 breast carcinoma cell targets (Fig. 4*B left* and *right*, respectively). Because our in vivo model employed a human tumor xenograft in mice, we also examined the mouse macrophage cell line ANA-1 as effector against human MDA-MB-231 target cells. Activated ANA-1 cells expressed constitutive cytotoxic activity against MDA-MB-231 cells in the presence of an iNOS inhibitor (0.5 mM aminoguanidine) to permit O_2^- accumulation (39). A 10-fold increase in tumoricidal activity was recorded after 12 h incubation with soluble TSP1 (5 μg/ml, Fig. 4*C*).

TSP1 has been shown to enhance chemoattractant fMLP-mediated superoxide generation in human neutrophils (14), suggesting that increased ROS mediates the tumoricidal activity of TSP1-stimulated cells. To confirm sensitivity to O_2^-, MDA-MB-231 cells were treated with xanthine and xanthine oxidase to generate O_2^-. Addition of O_2^- dose-dependently increased LDH release from the cells (Fig. 4*D*).

TSP1 increases extracellular release of O_2^-

To determine whether the known activity of TSP1 to enhance O_2^- release in human neutrophils extends to M1 differentiated U937 cells, IFNγ-differentiated U937 cells were stimulated with PMA (100 ng/ml), and O_2^- generation was assessed using luminol chemiluminiscence. Incubation of differentiated U937 cells with soluble TSP1 (20 μg/ml) significantly increased ($p \leq 0.001$) PMA-mediated O_2^- production (Fig. 5*A left*), 25 U of SOD completely abolished this signal (*data not shown*), confirming that O_2^- was responsible for the chemiluminescent signal. This also indicates that TSP1 stimulates extracellular O_2^- production because SOD does not degrade intracellular O_2^-. Similar enhancement of O_2^- generation by TSP1 was observed in monocytes isolated from human PBMCs and in a murine macrophage cell line ANA-1 (Fig. 5*A center-right*). Trimeric recombinant constructs (residues 1-356) containing the N-modules of TSP1 (NoC1) and TSP2 (residues 1-359, NoC2) but not other recombinant regions of TSP1 enhanced O_2^- production (Fig. 5*B*).

The N-module of TSP1 interacts with several receptors including α3β1, α4β1 and α6β1-integrins (40). Because α3β1-integrin recognizes the N-module of TSP1 but not TSP2 (41), we examined the role of α4β1 and α6β1-integrins. Differentiated U937 cells are known to express α4β1 (42), and we found that they also express α6β1 (Fig. 5*C*). The α6β1-binding peptide LALERKDHSG (24) and a function-blocking α6β1 antibody partially inhibited the activity of TSP1 on O_2^- generation. In contrast, the α4β1 antagonist phLDVP had no effect. These results identify a specific requirement for α6β1 integrin to mediate TSP1 binding to human monocytes and the subsequent activation of intracellular signaling pathways required for O_2^- production (Fig. 5*D right*).

TSP1-stimulated O_2^- production in macrophages requires intracellular Ca^{2+}

Ligation of some integrins triggers a transient elevation in intracellular free Ca^{2+} (43,44). Ca^{2+} is a second messenger for activation of NADPH oxidase in human monocytes (45). This result suggested that increased levels of Ca^{2+} might account for the enhancement by TSP1 of O_2^- production in differentiated U937 cells. Cells were loaded with Fluo-4 for 30 min and then treated with soluble TSP1 (20 μg/ml) for 25-50 min. Addition of TSP1 caused a significant rise in intracellular free Ca^{2+} (Fig. 6*A*). This increase was eliminated completely following chelation of extracellular Ca^{2+} by the addition of 1 mM EGTA (*data not shown*). To further confirm the role of Ca^{2+} in respiratory burst activity, differentiated U937 cells were treated with EGTA prior to the addition of PMA and TSP1. As shown in Fig. 6*B*, chelation of extracellular Ca^{2+} significantly decreased the stimulatory effect of TSP1 on PMA-mediated O_2^- generation in differentiated U937 cells, suggesting that a Ca^{2+} dependent mechanism is involved in TSP1 modulation of the macrophage respiratory burst.

Discussion

Several studies have suggested that TSP1 plays an important role in the recruitment of monocytes and macrophages to sites of tissue injury or inflammation (1,12). Here we provide evidence that over-expression of TSP1 in tumors increases macrophage recruitment *in vivo*. Tumor cells produce a range of chemotactic factors for macrophages. MCP-1 stimulates recruitment of macrophages into tumors *in vivo* (46), and decreased expression of this chemokines was reported to limit infiltration of macrophages into an excisional wound in TSP1

null mice (1). However, soluble TSP1 did not increase MCP-1 release from differentiated U937 human monocytic cells. PAI-1 is also required for cell migration *in vitro* (33), and evidence is emerging for a critical role of PAI-1 in macrophage migration *in vitro* and *in vivo* (32). TSP1 up-regulates PAI-1 in pancreatic cancer cells (47), and PAI-1 expression is up-regulated in TSP1-expressing MDA-MB-435 cells (34). We found that TSP1 acutely increased PAI-1 production by differentiated human and mouse macrophages, and strong TAM expression of PAI-1 was observed in TSP1 over-expressing tumors *in vivo*. This acute change in PAI-1 expression in response to TSP1 is at least partially TGFβ-mediated. Activation of latent TGFβ is mediated by the type 1 repeats of TSP1, but we found no induction of PAI-1 by this domain. Therefore, TSP1 probably induces PAI-1 via bound active TGFβ rather than activation of latent TGFβ produced by U937 cells. Although additional cytokines may be involved, autocrine induction of PAI-1 via tumor-cell produced TSP1 as well as paracrine induction of PAI-1 expression in TAMs could increase macrophage recruitment into the tumor.

Whether increased macrophage recruitment inhibits or enhances tumor growth depends on their differentiation state. The tumor environment can educate TAMs toward a tumor-promoting phenotype (M2) (18), which may prevent further macrophage migration within the tumor and ensure constant production of growth and angiogenic factors. In addition to contributing to macrophage infiltration by stimulating PAI-1 signaling in TAMs, we found that TSP1 expression in the tumor selectively increases M1 macrophage infiltration. This may provide a selective pressure distinct from its anti-angiogenic activity to account for the frequently observed down-regulation of TSP1 during tumor progression and its ability to inhibit tumor growth when re-expressed.

In general, M1 macrophages are efficient producers of reactive oxygen and nitrogen intermediates that mediate resistance against tumors (17). Here we provide evidence that tumor expression of TSP1 increases M1 polarization of TAMs assessed by iNOS expression. TSP1 was previously shown to enhance cytokine- and chemoattractant fMLP-induced respiratory burst in human neutrophils (13,14). We now demonstrate that TSP1 enhances PMA-mediated respiratory burst in U937 cells differentiated along an M1 pathway using IFN-γ. TSP1 stimulates the cytotoxic activity of differentiated human U937 cells and murine ANA-1 cells against several human breast carcinoma and melanoma cell lines. This contrasts with the reported activity of U937 cells to support tumor growth in an M2 manner when co-injected with prostate carcinoma cells (48). We found no effect of TSP1 on M2 differentiation of these cells in vitro. Therefore, U937 monocytes have the capacity to differentiate along both pathways, but TSP1 selectively enhances the cytotoxic effector function of M1 macrophages.

The N-terminal domains of TSP1 and TSP2 are sufficient for this priming activity but not for PAI-1 induction. The N-terminal domain of TSP1 mediates interactions with several integrin and non-integrin receptors (40). Differentiated U937 cells express α4β1 (42) and α6β1 integrins, and inhibition of α6β1 using a TSP1 peptide or a function-blocking α6β1 antibody provide evidence that this integrin mediates intracellular signaling pathways leading to increased O_2^- production.

Interactions between integrins and their ligands can trigger transient elevation in intracellular free Ca^{2+} (43,44), and Ca^{2+} is a well known intracellular second messenger for signaling the generation of O_2^- in human monocytes (45). We found that addition of TSP1 to differentiated U937 cells caused a significant increase in intracellular free Ca^{2+}, and that chelation of extracellular Ca^{2+} inhibits the stimulatory effect of TSP1 on mobilization of intracellular Ca^{2+} and PMA-mediated O_2^- generation in differentiated U937 cells. Taken together, these data suggest that a Ca^{2+}-dependent mechanism is involved in TSP1 modulation of the macrophage respiratory burst. However, we can not exclude the possibility that additional receptors recognized by the N-domains of TSP1 might contribute to O_2^- production by

macrophages. It is interesting that the N-terminal region of TSP2 shares this activity to stimulate O_2^- production by macrophages. Loss of TSP2 has also been noted with progression in some cancers, and over-expression of TSP2 limits tumor growth in murine models (19). Our data suggests this may involve both suppression of angiogenesis and enhancement of innate anti-tumor immunity.

Soluble TSP1 at 5 μg/ml was sufficient to increase U937-mediated cytotoxicity in all tumor cell targets tested. TSP1 was also reported to directly induce death of MDA-MB-231 and MCF-7 cells when used at 10 μg/ml for 24 h (49). Our results using a cytotoxicity assay based on LDH release showed minimal cytotoxic activity of soluble TSP1 against MDA-MB-231 cells, even after 72 h of incubation. Our data indicates that TSP1 stimulates macrophage-mediated tumor cell death due to accumulation of ROS. Physiologic doses of O_2^- generated using xanthine/xanthine oxidase were sufficient to inhibit MDA-MB-231 breast carcinoma cell viability.

In conclusion, the data presented here demonstrate that stimulation of M1 differentiated human monocytic cells with TSP1enhances tumor cell killing in vitro via production of reactive oxygen intermediates. In vivo, TSP1 promotes M1 macrophage recruitment into tumors while decreasing tumor growth. Clearly, TSP1 can also inhibit tumor growth via its anti-angiogenic activity, but our results suggest that TSP1 plays an additional role in tumor immunity by increasing M1 macrophage recruitment and cytotoxicity. Avoiding this innate immune surveillance could provide a second selective pressure to reduce TSP1 expression during tumor progression.

Acknowledgments

We thank Drs. Deane F. Mosher and Jack Lawler for providing reagents, Dr. Douglas D. Thomas for providing reagents and help with the ROS assay, and Russell W. Bandle for help with the intracellular calcium measurements.

This research was supported by the Intramural Research Program of the NIH, National Cancer Institute, Center for Cancer Research (MT, DAW, DDR). Gema Martin-Manso is recipient of a grant BEFI from Instituto de Salud Carlos III (Spanish Ministry of Heath).

References

1. Agah A, Kyriakides TR, Lawler J, Bornstein P. The lack of thrombospondin-1 (TSP1) dictates the course of wound healing in double-TSP1/TSP2-null mice. Am J Pathol 2002;161:831–9. [PubMed: 12213711]
2. Stenina OI, Byzova TV, Adams JC, McCarthy JJ, Topol EJ, Plow EF. Coronary artery disease and the thrombospondin single nucleotide polymorphisms. Int J Biochem Cell Biol 2004;36:1013–30. [PubMed: 15094117]
3. Crawford SE, Stellmach V, Murphy-Ullrich JE, et al. Thrombospondin-1 is a major activator of TGF-beta1 in vivo. Cell 1998;93:1159–70. [PubMed: 9657149]
4. Isenberg JS, Romeo MJ, Abu-Asab M, et al. Increasing survival of ischemic tissue by targeting CD47. Circ Res 2007;100:712–20. [PubMed: 17293482]
5. Roberts DD. Regulation of tumor growth and metastasis by thrombospondin-1. Faseb J 1996;10:1183–91. [PubMed: 8751720]
6. Ren Y, Savill J. Proinflammatory cytokines potentiate thrombospondin-mediated phagocytosis of neutrophils undergoing apoptosis. J Immunol 1995;154:2366–74. [PubMed: 7532668]
7. Moodley Y, Rigby P, Bundell C, et al. Macrophage recognition and phagocytosis of apoptotic fibroblasts is critically dependent on fibroblast-derived thrombospondin 1 and CD36. Am J Pathol 2003;162:771–9. [PubMed: 12598312]
8. Janabi M, Yamashita S, Hirano K, et al. Oxidized LDL-induced NF-kappa B activation and subsequent expression of proinflammatory genes are defective in monocyte-derived macrophages from CD36-deficient patients. Arterioscler Thromb Vasc Biol 2000;20:1953–60. [PubMed: 10938017]

9. Yamauchi Y, Kuroki M, Imakiire T, et al. Thrombospondin-1 differentially regulates release of IL-6 and IL-10 by human monocytic cell line U937. Biochem Biophys Res Commun 2002;290:1551–7. [PubMed: 11820799]
10. Suchard SJ. Interaction of human neutrophils and HL-60 cells with the extracellular matrix. Blood Cells 1993;19:197–221. [PubMed: 7508769]
11. Mansfield PJ, Boxer LA, Suchard SJ. Thrombospondin stimulates motility of human neutrophils. J Cell Biol 1990;111:3077–86. [PubMed: 2269666]
12. Mansfield PJ, Suchard SJ. Thrombospondin promotes chemotaxis and haptotaxis of human peripheral blood monocytes. J Immunol 1994;153:4219–29. [PubMed: 7930624]
13. Nathan C, Srimal S, Farber C, et al. Cytokine-induced respiratory burst of human neutrophils: dependence on extracellular matrix proteins and CD11/CD18 integrins. J Cell Biol 1989;109:1341–9. [PubMed: 2475511]
14. Suchard SJ, Boxer LA, Dixit VM. Activation of human neutrophils increases thrombospondin receptor expression. J Immunol 1991;147:651–9. [PubMed: 1712815]
15. Majluf-Cruz A, Manns JM, Uknis AB, et al. Residues F16-G33 and A784-N823 within platelet thrombospondin-1 play a major role in binding human neutrophils: evaluation by two novel binding assays. J Lab Clin Med 2000;136:292–302. [PubMed: 11039850]
16. Lewis CE, Pollard JW. Distinct role of macrophages in different tumor microenvironments. Cancer Res 2006;66:605–12. [PubMed: 16423985]
17. Mantovani A, Sica A, Locati M. New vistas on macrophage differentiation and activation. Eur J Immunol 2007;37:14–6. [PubMed: 17183610]
18. Pollard JW. Tumour-educated macrophages promote tumour progression and metastasis. Nat Rev Cancer 2004;4:71–8. [PubMed: 14708027]
19. Carlson CB, Lawler J, Mosher DF. Structures of thrombospondins. Cell Mol Life Sci 2008;65:672–86. [PubMed: 18193164]
20. Roberts DD, Cashel J, Guo N. Purification of Thrombospondin from human platelets. J Tissue Cult Methods 1994;16:217–22.
21. Misenheimer TM, Huwiler KG, Annis DS, Mosher DF. Physical characterization of the procollagen module of human thrombospondin 1 expressed in insect cells. J Biol Chem 2000;275:40938–45. [PubMed: 11016937]
22. Miao WM, Seng WL, Duquette M, Lawler P, Laus C, Lawler J. Thrombospondin-1 type 1 repeat recombinant proteins inhibit tumor growth through transforming growth factor-beta-dependent and -independent mechanisms. Cancer Res 2001;61:7830–9. [PubMed: 11691800]
23. Anilkumar N, Annis DS, Mosher DF, Adams JC. Trimeric assembly of the C-terminal region of thrombospondin-1 or thrombospondin-2 is necessary for cell spreading and fascin spike organisation. J Cell Sci 2002;115:2357–66. [PubMed: 12006620]
24. Calzada MJ, Sipes JM, Krutzsch HC, et al. Recognition of the N-terminal modules of thrombospondin-1 and thrombospondin-2 by alpha6beta1 integrin. J Biol Chem 2003;278:40679–87. [PubMed: 12909644]
25. Lin K, Ateeq HS, Hsiung SH, et al. Selective, tight-binding inhibitors of integrin alpha4beta1 that inhibit allergic airway responses. J Med Chem 1999;42:920–34. [PubMed: 10072689]
26. Weinstat-Saslow DL, Zabrenetzky VS, VanHoutte K, Frazier WA, Roberts DD, Steeg PS. Transfection of thrombospondin 1 complementary DNA into a human breast carcinoma cell line reduces primary tumor growth, metastatic potential, and angiogenesis. Cancer Res 1994;54:6504–11. [PubMed: 7527299]
27. Sundstrom C, Nilsson K. Establishment and characterization of a human histiocytic lymphoma cell line (U-937). Int J Cancer 1976;17:565–77. [PubMed: 178611]
28. Cox GW, Mathieson BJ, Gandino L, Blasi E, Radzioch D, Varesio L. Heterogeneity of hematopoietic cells immortalized by v-myc/v-raf recombinant retrovirus infection of bone marrow or fetal liver. J Natl Cancer Inst 1989;81:1492–6. [PubMed: 2778838]
29. Guo NH, Krutzsch HC, Inman JK, Shannon CS, Roberts DD. Antiproliferative and antitumor activities of D-reverse peptides derived from the second type-1 repeat of thrombospondin-1. J Pept Res 1997;50:210–21. [PubMed: 9309585]

30. Rae JM, Creighton CJ, Meck JM, Haddad BR, Johnson MD. MDA-MB-435 cells are derived from M14 melanoma cells--a loss for breast cancer, but a boon for melanoma research. Breast Cancer Res Treat 2007;104:13–9. [PubMed: 17004106]

31. Lu B, Rutledge BJ, Gu L, et al. Abnormalities in monocyte recruitment and cytokine expression in monocyte chemoattractant protein 1-deficient mice. J Exp Med 1998;187(4):601–8. [PubMed: 9463410]

32. Cao C, Lawrence DA, Li Y, et al. Endocytic receptor LRP together with tPA and PAI-1 coordinates Mac-1-dependent macrophage migration. Embo J 2006;25:1860–70. [PubMed: 16601674]

33. Degryse B, Neels JG, Czekay RP, Aertgeerts K, Kamikubo Y, Loskutoff DJ. The low density lipoprotein receptor-related protein is a motogenic receptor for plasminogen activator inhibitor-1. J Biol Chem 2004;279:22595–604. [PubMed: 15001579]

34. Albo D, Rothman VL, Roberts DD, Tuszynski GP. Tumour cell thrombospondin-1 regulates tumour cell adhesion and invasion through the urokinase plasminogen activator receptor. Br J Cancer 2000;83:298–306. [PubMed: 10917542]

35. Song CZ, Siok TE, Gelehrter TD. Smad4/DPC4 and Smad3 mediate transforming growth factor-beta (TGF-beta) signaling through direct binding to a novel TGF-beta-responsive element in the human plasminogen activator inhibitor-1 promoter. J Biol Chem 1998;273:29287–90. [PubMed: 9792626]

36. Murphy-Ullrich JE, Schultz-Cherry S, Hook M. Transforming growth factor-beta complexes with thrombospondin. Mol Biol Cell 1992;3:181–8. [PubMed: 1550960]

37. Young GD, Murphy-Ullrich JE. The tryptophan-rich motifs of the thrombospondin type 1 repeats bind VLAL motifs in the latent transforming growth factor-beta complex. J Biol Chem 2004;279:47633–42. [PubMed: 15342643]

38. Munder M, Eichmann K, Modolell M. Alternative metabolic states in murine macrophages reflected by the nitric oxide synthase/arginase balance: competitive regulation by CD4+ T cells correlates with Th1/Th2 phenotype. J Immunol 1998;160:5347–54. [PubMed: 9605134]

39. Thomas DD, Ridnour LA, Espey MG, et al. Superoxide fluxes limit nitric oxide-induced signaling. J Biol Chem 2006;281:25984–93. [PubMed: 16829532]

40. Calzada MJ, Roberts DD. Novel integrin antagonists derived from thrombospondins. Curr Pharm Des 2005;11:849–66. [PubMed: 15777239]

41. Calzada MJ, Zhou L, Sipes JM, et al. Alpha4beta1 integrin mediates selective endothelial cell responses to thrombospondins 1 and 2 in vitro and modulates angiogenesis in vivo. Circ Res 2004;94:462–70. [PubMed: 14699013]

42. Prieto J, Eklund A, Patarroyo M. Regulated expression of integrins and other adhesion molecules during differentiation of monocytes into macrophages. Cell Immunol 1994;156:191–211. [PubMed: 8200035]

43. Jaconi ME, Theler JM, Schlegel W, Appel RD, Wright SD, Lew PD. Multiple elevations of cytosolic-free Ca2+ in human neutrophils: initiation by adherence receptors of the integrin family. J Cell Biol 1991;112:1249–57. [PubMed: 1900302]

44. Coppolino MG, Woodside MJ, Demaurex N, Grinstein S, St-Arnaud R, Dedhar S. Calreticulin is essential for integrin-mediated calcium signalling and cell adhesion. Nature 1997;386:843–7. [PubMed: 9126744]

45. Scully SP, Segel GB, Lichtman MA. Relationship of superoxide production to cytoplasmic free calcium in human monocytes. J Clin Invest 1986;77:1349–56. [PubMed: 3007579]

46. Hoshino Y, Hatake K, Kasahara T, et al. Monocyte chemoattractant protein-1 stimulates tumor necrosis and recruitment of macrophages into tumors in tumor-bearing nude mice: increased granulocyte and macrophage progenitors in murine bone marrow. Exp Hematol 1995;23:1035–9. [PubMed: 7635182]

47. Albo D, Berger DH, Vogel J, Tuszynski GP. Thrombospondin-1 and transforming growth factor beta-1 upregulate plasminogen activator inhibitor type 1 in pancreatic cancer. J Gastrointest Surg 1999;3:411–7. [PubMed: 10482694]

48. Craig M, Ying C, Loberg RD. Co-inoculation of prostate cancer cells with U937 enhances tumor growth and angiogenesis in vivo. J Cell Biochem 2008;103:1–8. [PubMed: 17541941]

49. Manna PP, Frazier WA. CD47 mediates killing of breast tumor cells via Gi-dependent inhibition of protein kinase A. Cancer Res 2004;64:1026–36. [PubMed: 14871834]

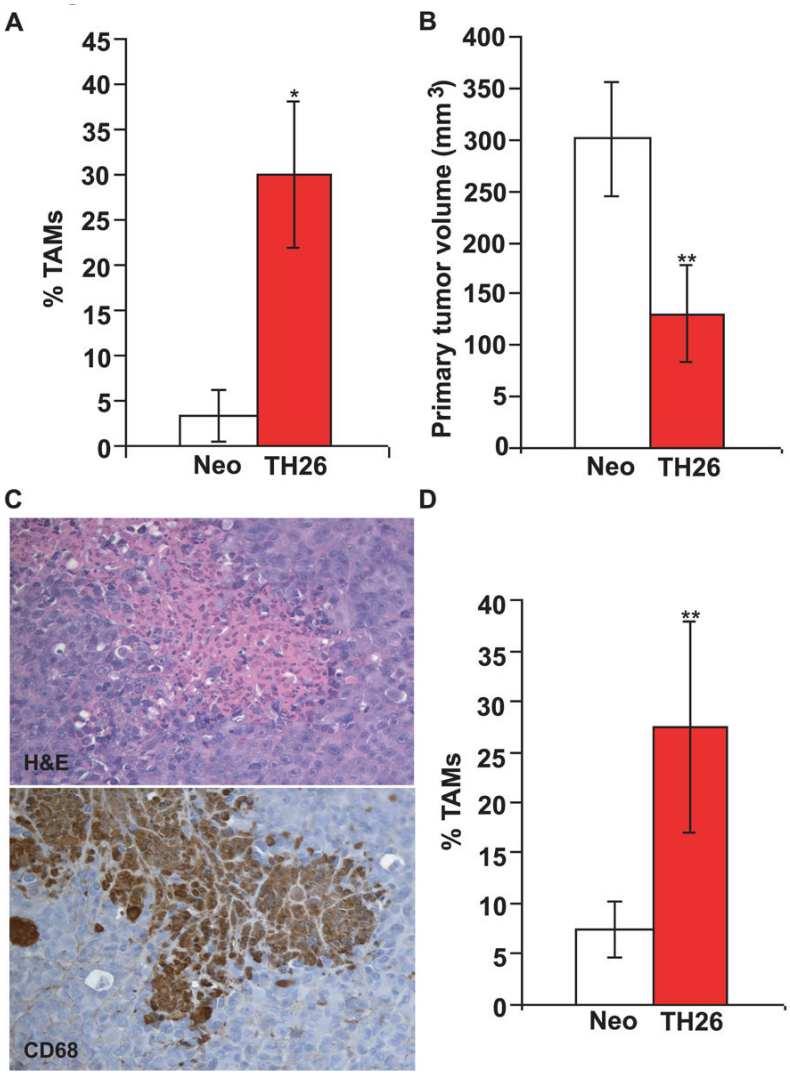

Figure 1.

*THBS*1 over-expression promotes macrophage recruitment in tumor-bearing nude mice. *A*, Tissue sections cut from paraffin-embedded tumors harvested from NIH-*bg/nu* mice injected in the mammary fat pads with TH26 or Neo MDA-MB-435 clones were stained with Hematoxylin-Eosin and rat anti-mouse CD68 antibody (clone FA-11). Quantitative analysis of macrophage infiltration into the tumor specimens was performed by evaluating the number of CD68-positive cells per 100x field in non-necrotic areas. The results are presented as a percentage of TAMs in Neo control (*white columns*) versus *THBS1*-transfected TH26 tumors (*red columns*). *B*, primary tumor size 24 days post-injection in NIH-*nu/nu* mice given subcutaneous injections of TH26 (*red columns*) or Neo cells (*white columns*). Histogram represents the tumor volume (mm^3) of all animals within each group that developed a tumor. *C*, Paraffin-embedded sections cut from clone TH26 tumors grown subcutaneously in NIH-*nu/nu* mice were stained with Hematoxylin-Eosin (*top*) and rat anti-mouse CD68 antibody (clone FA-11) (*bottom*). Representative photomicrographs of adjacent slides are shown from experiments conducted in tumor samples from 12 NIH-*nu/nu* mice. Three mice did not develop tumors. Identical patterns were observed in all of the tumors examined. Magnification, x200. *D*, quantitative analysis of macrophage infiltration into subcutaneous tumors grown in NIH-*nu/nu* mice was evaluated as the percent of CD68-positive cells in multiple 100x fields in non-

necrotic areas. The results are presented as a percentage of TAMs in Neo (*white column*) and TH26 tumors (*red column*).

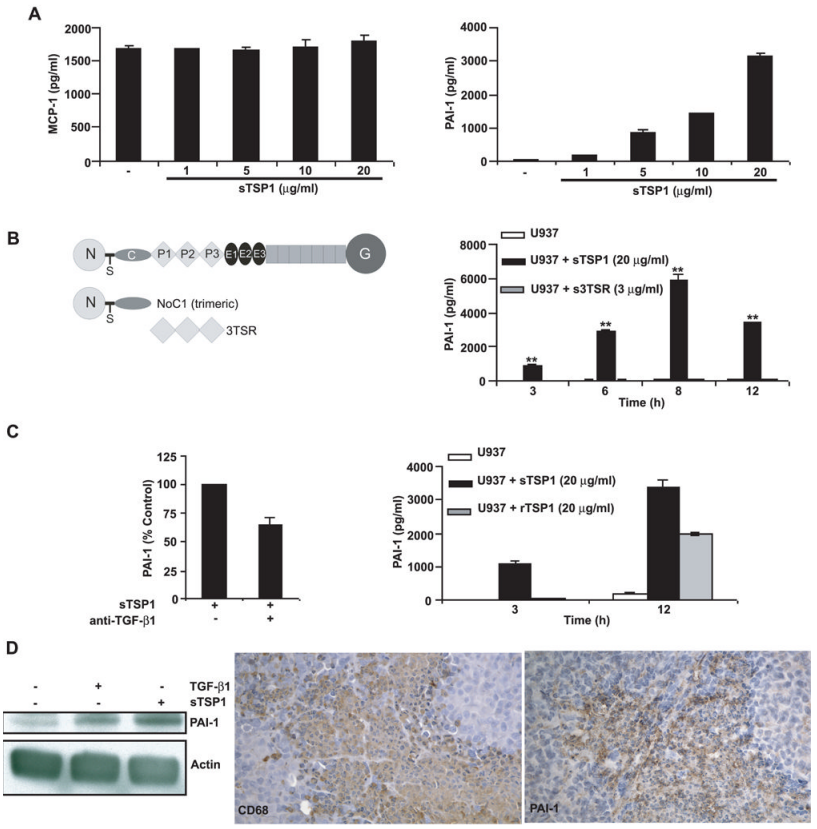

Figure 2.

Effects of TSP1 on MCP-1 and PAI-1 expression in differentiated U937 human monocytic cells and mouse macrophages. *A-C*, differentiated U937 cells (1×10^6/0.5 ml RPMI 1640 with 0.5% FBS) were incubated in the absence or the presence of soluble TSP1, soluble recombinant type 1 repeats of TSP1 (3TSR, *B*), or soluble recombinant human TSP1 (*C right*). After 12 h incubation (*A*), or at the indicated times (*B-C right*), the supernatants were harvested, and total MCP-1 and PAI-1 were determined using a multiplexed ELISA array (Quansys Biosciences), as described in *Materials* and *Methods*. Data are representative of at least four different experiments. *C left*, differentiated U937 cells were incubated with neutralizing TGFβ1 antibody (*clone 9016*) for 15 min before the addition of soluble TSP1 (20μg/ml). Culture supernatants collected after 12 h were used to measure total PAI-1. Data are representative of two different experiments. *D left*, serum-deprived murine RAW264.7 cells were stimulated with TGFβ1 (1 ng/ml), as a positive control, or soluble TSP1 (20 μg/ml) for 2 h. The experiment was repeated three times, and a representative anti-PAI-1 blot is shown. Actin was used to confirm equal protein loading. *D right*, Paraffin-embedded sections cut from TH26 tumors grown subcutaneously in NIH-*nu/nu* mice were stained with rat anti-mouse CD68 antibody (clone FA-11) (*left*) and rabbit anti-mouse PAI-1 antibody (*right*). Representative photomicrographs of adjacent sections are shown from experiments conducted in tumor samples from 12 NIH-*nu/nu* mice. Identical patterns were observed in all of the tumors examined. Magnification, x200.

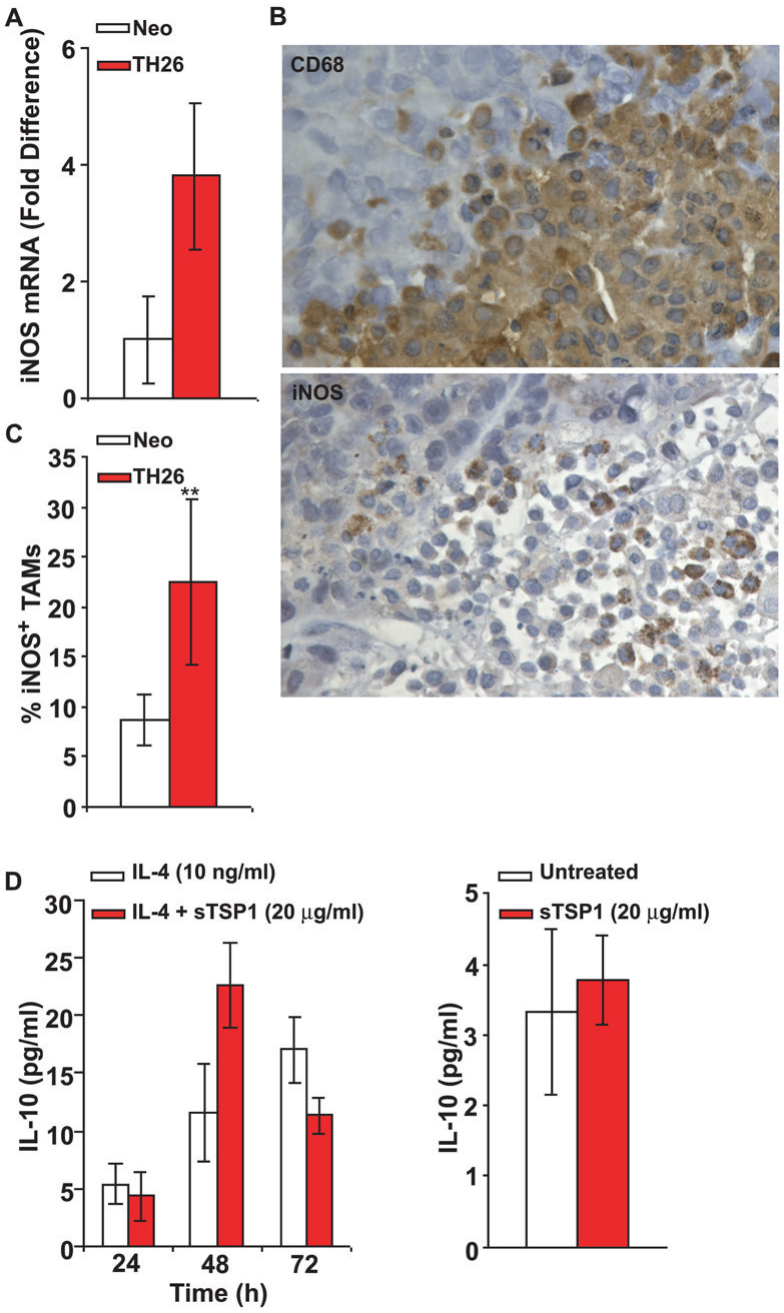

Figure 3.

Increased iNOS-expressing M1 TAMs in TSP1 over-expressing tumors. *A*, Real-time quantitative reverse transcription-PCR analysis of mRNA expression in TH26 and Neo tumors from 6 NIH-*nu/nu* mice. Fold difference was adjusted to HPRT1 internal control values. Relative quantification of iNOS was calculated by the $2^{\Delta\Delta CT}$ method. *B*, Immunohistochemical analysis of TH26 and Neo tumors in NIH-*nu/nu* mice. Adjacent sections were stained using rat anti-mouse CD68 antibody (clone FA-11) (*top*) and rabbit polyclonal antibody to iNOS to detect M1 differentiated TAMs (*bottom*). The results are representative of tumor samples from 12 NIH-*nu/nu* mice, which showed identical patterns. Magnification, x400. *C*, Quantitative analysis of CD68-positive cells expressing iNOS in the tumor specimens was performed by

evaluating the percentage of iNOS-positive macrophages in multiple 100x fields. The results are presented as the percentage of iNOS-positive TAMs in Neo control (*white columns*) and TH26 tumors (*red columns*). *D left*, U937 cells (2×10^5/0.5 ml AIM-V) were incubated with IL-4 to induce M2 differentiation in the absence or the presence of soluble TSP1. At the indicated times, the supernatants were harvested, and IL-10 was determined using a Multiplexed ELISA array (Quansys Biosciences) as described in *Materials* and *Methods*. *D right*, U937 cells were differentiated with IL-4 for 72 h, and then the differentiated cells (1×10^6/1 ml AIM-V) were incubated with soluble TSP1. After 12 h incubation, the supernatants were harvested, and IL-10 was determined using a Multiplexed ELISA array.

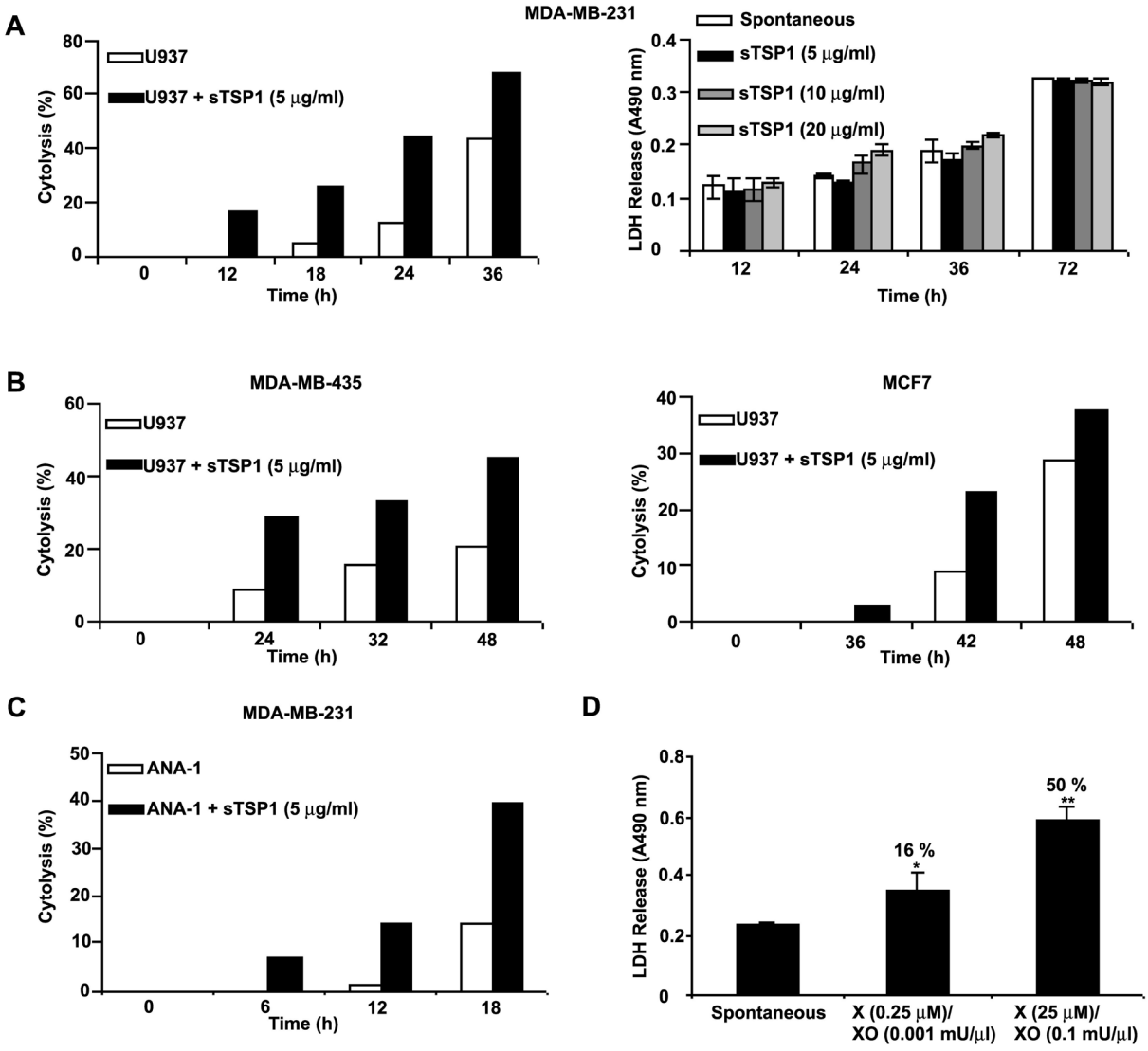

Figure 4.

TSP1 increases U937 human monocytic cell-mediated tumoricidal activity. *A left-B*, MDA-MB-231, MDA-MB-435, and MCF-7 target cells (2×10^4/150 μl RPMI 1640 with 10 % FBS) were seeded into 16-well sensor plates and incubated for up to 24 h. After this incubation, differentiated U937 effector cells (8×10^5/50 μl RPMI 1640 with 10 % FBS) were directly added into wells containing target cells, in the absence or the presence of soluble TSP1. The measurements were automatically collected by the analyzer RT-CES system (ACEA Biosciences) for up to 48 h. Data are representative of three different experiments. *A right*, MDA-MB-231 cells (2×10^4/200 μl RPMI 1640 with 10 % FBS) were seeded into 96-well plates and incubated for up to 72 h in the absence or the presence of soluble TSP1 (5-20 μg/ml). At the indicated times, medium samples were collected and LDH released was measured as described in *Materials* and *Methods*. The absorbance was recorded at 490 nm. Data are representative of two different experiments. *C*, MDA-MB-231 target cells (2×10^4/150 μl RPMI 1640 with 10 % FBS) were seeded into 16-well sensor plates and incubated for up to 24 h. After this incubation, activated ANA-1 effector cells (8×10^5/50 μl RPMI 1640 with 10 % FBS and 0.5 mM aminoguanidine) were directly added into wells containing target cells, in the absence or the presence of soluble TSP1. The measurements were automatically collected

by the RT-CES system for up to 18 h. Data are representative of four different experiments. *D*, MDA-MB-231 target cells (2,500cells/100 μl RPMI 1640 with 1.25 % FBS) were seeded into 96-well plates and incubated for 72 h in the absence or the presence of different doses of xanthine and xanthine oxidase. The medium samples were collected, and LDH released was measured. The absorbance was recorded at 490 nm. The percentage of cytotoxicity is shown above each bar and is calculated as (Experimental-Spontaneous/Maximum-Spontaneous) x100. Maximum LDH release was determined by complete lysis of target cells.

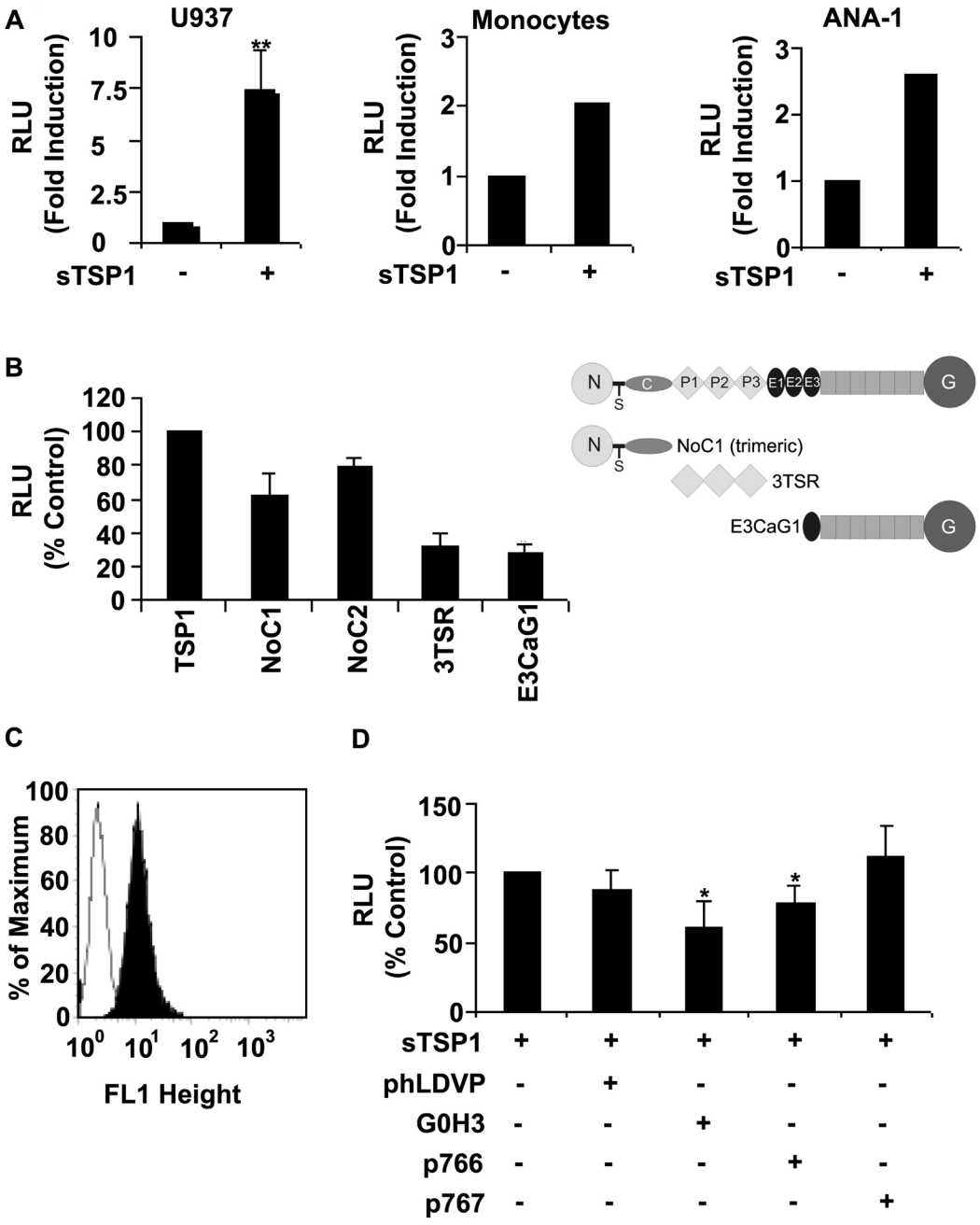

Figure 5.

TSP1 enhances extracellular release of O_2^- in human and mouse monocytic cells. *A* (*left*), differentiated U937 cells (5×10^5/condition) were stimulated with PMA (100 ng/ml) in the absence or presence of soluble TSP1 (20 μg/ml) for up to 70 min, and quantitative analysis of O_2^- levels was performed with a LumiMax Superoxide Anion detection kit (Stratagene) and quantified using a luminometer. The results are presented as the ratio maximum activity (relative luminescence units, RLU)/min. The data represent the mean ± SD of five different experiments. *A* (*center*), analysis of O_2^- release from human monocytic cells. Monocytes obtained from human PBMCs (5×10^5/condition) were stimulated with PMA (10 ng/ml) in the absence or the presence of soluble TSP1 (20 μg/ml) for 30 min. The results are presented

as the ratio maximum activity (RLU)/min. Data are representative of four different experiments. *A* (*right*), activated ANA-1 cells (8×10^5/condition) were stimulated with PMA (100 ng/ml) and aminoguanidine (0.5 mM) in the absence or the presence of soluble TSP1 (5 μg/ml) for 130 min. The results are presented as RLU and are representative of two different experiments. *B*, analysis of O_2^- release from differentiated U937 cells (5×10^5/condition) stimulated as described above in the absence or the presence of soluble TSP1 (20 μg/ml), NoC1, 3TSR, or E3CaG1 (10 μg/ml) for up to 40 min. The results are presented as a % of control RLU determined in the presence of TSP1 and represent the mean ± SD of up to four different experiments. *C*, surface α_6-integrin expression in differentiated U937 cells was analyzed using flow cytometry, as described in *Materials* and *Methods*. *D*, analysis of O_2^- release from differentiated U937 cells (5×10^5/condition) stimulated as described above with soluble TSP1 (20 μg/ml) in the absence or the presence of the $\alpha_4\beta_1$ integrin antagonist phLDVP (1 μM), the function-blocking rat anti-human α_6 monoclonal antibody (clone G0H3)(5 μg/ml), p766, or control peptide (p767, 200 μM) for up to 40 min. The results are presented as a % of control RLU determined in the presence of TSP1 alone and represent the mean ± SD of up to five different experiments.

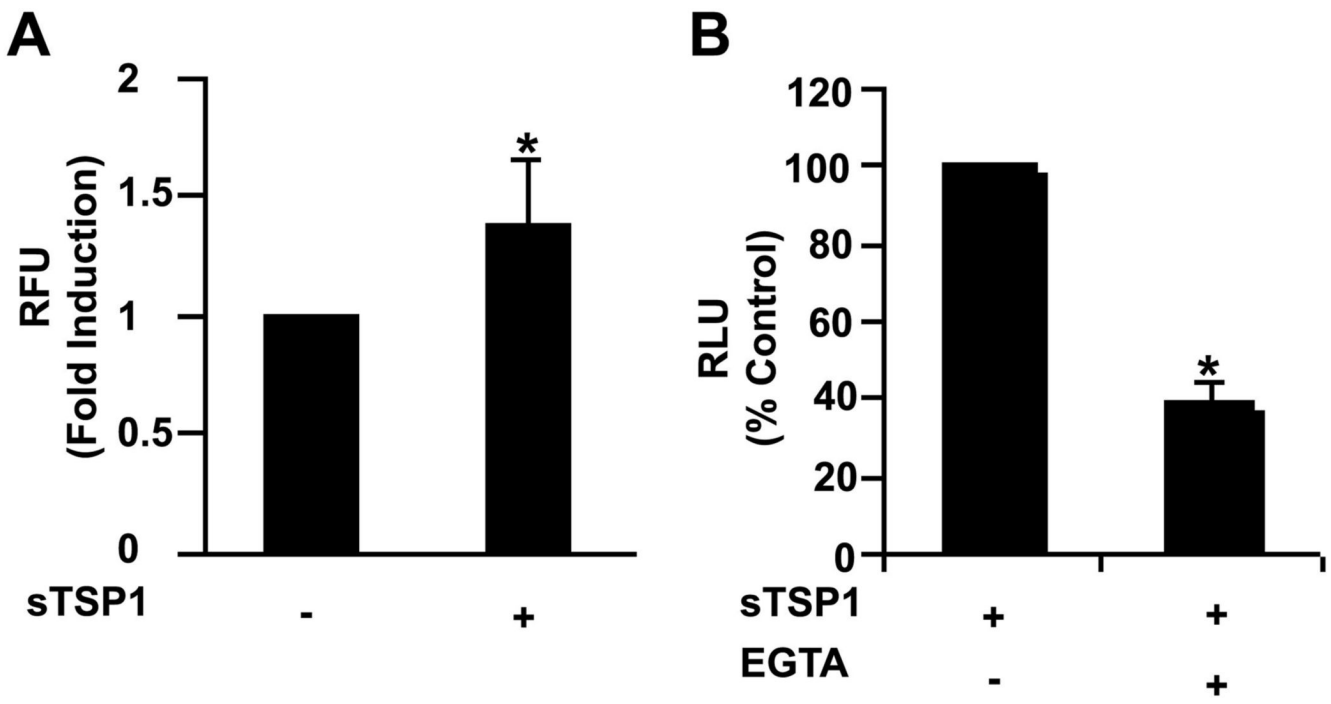

Figure 6.

Ca^{2+} is an intracellular second messenger for activation of the oxidative burst in TSP1-stimulated U937 monocytic cells. *A*, analysis of intracellular free Ca^{2+} was performed in differentiated U937 cells. U937 (4×10^5 cells/condition) were loaded with Fluo-4 for 30 min and then treated with soluble TSP1 (20 μg/ml), as described in *Materials* and *Methods*. The cells were then placed in a fluorometer and measurements were acquired for 40 min. Results are presented as fold induction in TSP1 treated (+) relative to untreated cells (−). The data represent the mean ± SD of four different experiments. *B*, analysis of O_2^- release from differentiated U937 cells (5×10^5/condition) stimulated with PMA (100 ng/ml) and soluble TSP1 (20 μg/ml) in the absence or the presence of EGTA (1 mM) for up to 45 min. The levels of O_2^- were determined by luminescence as described in Figure 5. The results are presented as a % of control RLU determined in the presence of TSP1 alone and are representative of two different experiments.